

# Mathematical Modelling of Sound Radiation from a T Junction of City Roads in Windy Conditions

Olexa PIDUBNIAK<sup>(1)</sup>, Nadia PIDUBNIAK<sup>(2)</sup>

<sup>(1)</sup> Faculty of Process and Environmental Engineering  
Lodz University of Technology  
Wólczajska 213, 90-924 Łódź, Poland; e-mail: piddub@wp.pl

<sup>(2)</sup> Lviv, Ukraine

(received March 8, 2016; accepted May 16, 2016)

The sound radiation from vehicles travelling on the city roads with T junction was considered. The wind effect on acoustic field was taken into account. The solution of this problem was found with the help of the integral Fourier transforms and stationary phase method as the superposition of solutions for the cases of vehicles moving along the straight roads and roads with right-angle bend. As an example, the numerical analysis of traffic noise characteristics was carried out for the T junction city road on one of streets in the town of Łódź (Poland).

**Keywords:** T junction of city roads; traffic noise propagation; stationary phase method; acoustic pressure; power flow density.

## 1. Introduction

The communication noise depends not only on types of its sources but in large measure of roads geometry, on which the transport vehicles move. The geometry of city roads as a rule is characterized by the straight lines of motion, bends, roundabouts and cross-roads different types. These road elements influence, under certain conditions, forming the structure of acoustic field radiated from moving cars and other transport facilities. T junction of the roads is one of many elements of city streets too. With changes in the direction of cars motion, this element is the important source of noise. Noise generated at T junction bend must be different from the noise generated by cars travelling on straight road. However, theoretical investigations of this field of acoustic environment have been insufficiently developed yet.

The last years researchers directed their attention to developing of new noise prediction models founded on the data measurement and empirical approaches for case of noise generation on the complicated road intersections with variable traffic dynamics. Thus, CHEVALIER *et al.* (2009a) described and critically analyzed three types of road noise prediction models (static,

analytic and micro-simulation models) for the problem of noise levels determination at road crossings. It was shown that the micro-simulation packages which couple microscopic traffic simulation tool with noise emission laws and sound propagation algorithms, were effective above all. HALLIWELL (1980) studied the effect of stop signs and traffic lights on the noise level. It was revealed a small but measurable increase of noise level in the vicinity of roadways intersection and road T junction. JAHANDAR *et al.* (2012) investigated traffic noise on most critical areas near the intersections, crossroads and T junctions and reached the similar conclusion. YOSHIHISA *et al.* (2004) asserted on the base of their results of measurements that noise level at roadsides was almost independent of the distance from intersection. The strong influence of geometry and general features of the road on forming of vehicular flow noise was also shown (GUARNACCIA, 2010). The methods for predicting noise with taken into account effects of vehicle acceleration and deceleration by signals on intersection zone was developed also by NAMIKAWA *et al.* (2010). The distribution of noise level near roads junction which reminds T junction was investigated using the theoretical consideration and modelling vehicular flow by the electrical current. SYKES, DREW

(2011) described the using software library and experimental data for computer micro-simulation traffic noise levels near and far from the signalized road T junctions and studied the effects of speed and accelerating traffic flows on noise and also summation effect of noise from the several vehicles. MAKAREWICZ, KOKOWSKI (2007) and COVACIU *et al.* (2013) also investigated the speed and acceleration of vehicles causing traffic noise near roundabout and road junctions. It was denoted on the importance of accuracy in collecting traffic data for the analysis of noise levels distribution near these elements of roads. CYRIL, KOSHY (2013) consisted short historical excursus in the development of road traffic noise models. On the base of the collected data authors constructed the statistical regression model for traffic noise predicting on the T junction of roads.

The problem in modelling of the conflict-free routes on a signalled T junction, closely constrained with the investigation of traffic noise, was raised by FOTHERBY (2002). Similarly, the optimal signalization and stop-control procedures regulation of the traffic flow on roundabout and road T junction were developed (CHODUR, 2007; MOHYLA *et al.*, 2013; JOHNSON, 2014).

This short review of publications and their analysis shows that many different models for description of noise impact around intersections and roundabouts were proposed and discussed. However, as the result of complexity of the problem, many of these works are based on the empirical and technical acoustical models with minimum application of the mathematical physics apparatus.

Recently, the attention of researchers on this subject was focused on the problems of mathematical modelling of noise generated from particular elements of city streets and roads. So, it was carried out studying the case, in which cars move on straight multi-lines road taking into account velocity and direction of wind (PIDUBNIAK *et al.*, 2009b). The similar research was fulfilled for controlled cross-roads (PIDUBNIAK *et al.*, 2009a). The models of sound propagation from passenger cars and trucks moving on roundabout were proposed by MAKAREWICZ, GOLEBIEWSKI (2007), CHEVALLIER *et al.* (2009b) and PIDUBNIAK, PIDUBNIAK (2010). The effect of right-angle bend in the road on noise level was investigated by ZHAO *et al.* (2012) and PIDUBNIAK *et al.* (2012a). Our investigations of noise on straight road (including the case of road intersections), roundabout and road with a right-angle bend became the base for mathematical modelling of sound generation from vehicles moving on the road T and Y junctions (see shorts reports that have thesis character: PIDUBNIAK *et al.*, 2013; 2014).

The main goal of this work was to formulate more profoundly and numerically realized the asymptoti-

cally exact analytical algorithm for analysis of acoustic pressure and power flow density caused by many vehicles travelling in two mutually opposite directions on city dual-carriageway road with T junction in windy conditions.

## 2. The problem statement and method for its solution

Let us consider the problem of sound radiation from moving motor vehicles on the elements of road, geometric characteristics of which are represented in Fig. 1. In this figure the six lines with directions of vehicles motion are shown. These vehicles as passenger cars ( $L$ ) and trucks ( $C$ ) moved, respectively, with constant velocities  $v_L$  and  $v_C$ . The intervals between vehicles  $\Delta_L$  and  $\Delta_C$  are invariable. We considered the vehicles as the point sound sources with frequencies  $\Omega_L$  and  $\Omega_C$  wafting in the acoustic medium parallel to road surface on constant heights  $z = h_L$  and  $z = h_C$  ( $h_L < h_C$ ) with force vector intensities  $\mathbf{F}_L$  and  $\mathbf{F}_C$ . It was assumed that acoustic medium moves parallel to the road plane with constant velocity  $\mathbf{v}_w$  in direction  $\theta = \theta_w$  to axis  $0x$ :  $\mathbf{v}_w = (v_{wx}, v_{wy}, 0)$ ;  $v_{wx} = v_w \cos \theta_w$ ,  $v_{wy} = v_w \sin \theta_w$ ,  $v_w = |\mathbf{v}_w|$ .

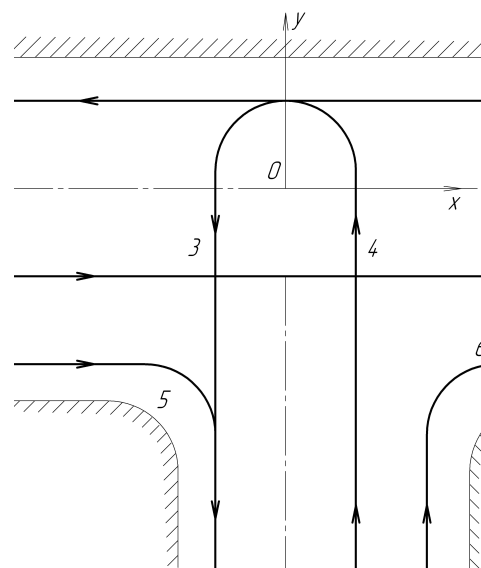


Fig. 1. Configuration of T intersection of city roads in system of coordinates  $0xy$  with six passenger cars and trucks moving lines.

As follows from Fig. 1 we had to deal with three types of road lanes (Figs. 2a, b, c).

From the mathematical point of view the problem consisted in solution of system of equations of acoustics for a half-space over road ( $z > 0$ ) and equations of dynamic elasticity theory for a half-space under road ( $z < 0$ ) taking into consideration junction conditions of acoustic and elastic media on surface  $z = 0$ . The basic relations for linear acoustics of the moving media

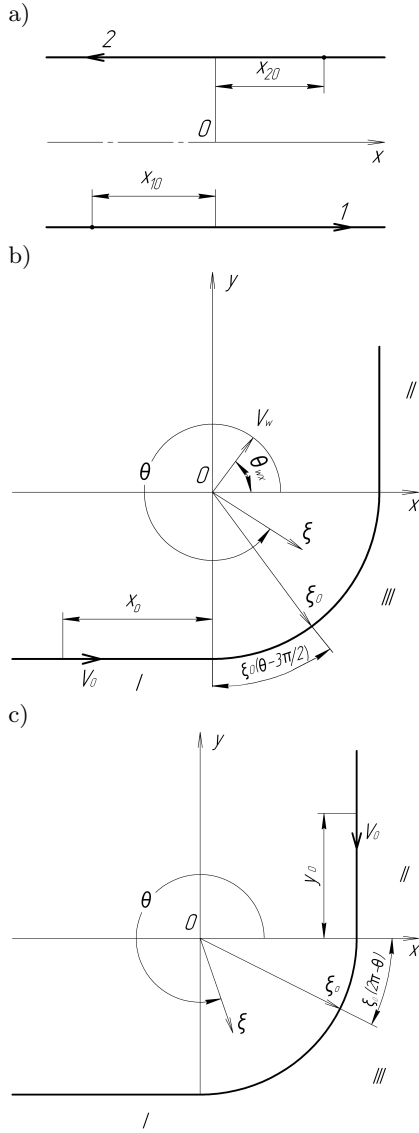


Fig. 2. Scheme of transference of point sound sources along straight lines and curve lines with the local system of polar coordinates  $(\xi, \theta)$ : a) source motion forward (1) and back (2) on straight lines; b) source motion in counter-clockwise direction; c) source motion in clockwise direction;  $(x_{10}, x_{20}, x_0, y_0)$  are coordinates of point sound sources locations in certain moment of motion).

are equations of motion and mass balance (MORSE, INGART, 1968):

$$\begin{aligned} \rho \frac{d\mathbf{v}(\mathbf{x}, t)}{dt} &= -\nabla p(\mathbf{x}, t) + \mathbf{F}(\mathbf{x}, t), \\ \nabla \cdot \mathbf{v}(\mathbf{x}, t) &= -\frac{1}{\rho c^2} \frac{dp(\mathbf{x}, t)}{dt}, \end{aligned} \quad (1)$$

where  $p(\mathbf{x}, t)$  is the acoustic pressure,  $\mathbf{v}(\mathbf{x}, t)$  is the particle velocity,  $\rho$  is the acoustic density,  $c$  is the sound

velocity,  $t$  is the time,  $\nabla$  is the Hamilton operator,  $\nabla = \nabla_{\perp} + \mathbf{i}_z \partial / \partial z$ , where  $\nabla_{\perp} = \mathbf{i}_x \partial / \partial x + \mathbf{i}_y \partial / \partial y$ ,  $\mathbf{i}_x, \mathbf{i}_y, \mathbf{i}_z$  are the unit vectors. The global derivative with respect to time is determined as  $d/dt \equiv \partial / \partial t + \mathbf{v}_w \cdot \nabla_{\perp}$ . It should be noted that the particle velocity vector is connected with particle displacement vector in moving acoustic medium by the relation:

$$\mathbf{v}(\mathbf{x}, t) = d\mathbf{u}(\mathbf{x}, t) / dt = \partial \mathbf{u}(\mathbf{x}, t) / \partial t + \mathbf{v}_w \cdot \nabla_{\perp} \mathbf{u}(\mathbf{x}, t).$$

In Eqs. (1)  $\mathbf{F}(\mathbf{x}, t)$  is the complex mass load vector,  $\mathbf{F}(\mathbf{x}, t) = \mathbf{F}_0 G(\boldsymbol{\xi}, t) \delta(z - z_0)$ , where  $\mathbf{F}_0$  is the vector of constant mass load real amplitudes,  $\delta(z)$  is the Dirac function,  $G(\boldsymbol{\xi}, t)$  is the function characterized complex mass load distribution in plane  $Oxy$ ;  $\mathbf{x} = \boldsymbol{\xi} + \mathbf{i}_z z$  and  $\boldsymbol{\xi} = \mathbf{i}_x x + \mathbf{i}_y y$  are the radius-vectors in space  $Oxyz$  and plane  $Oxy$ , respectively.

On the acoustic medium – elastic half-space interface ( $z = 0$ ) the following conditions satisfy:

$$\sigma_z + p_{\text{tot}} = 0, \quad \tau_{xz} = 0, \quad \tau_{yz} = 0, \quad u_{sz} = u_{\text{tot},z},$$

where  $p_{\text{tot}} = p_{\text{rad}} + p_{\text{ref}}$ ,  $u_{\text{tot},z} = u_{\text{rad},z} + u_{\text{ref},z}$  are the total acoustic pressure and total normal component of particle displacement vector in acoustic medium  $z > 0$ , respectively,  $\sigma_z, \tau_{xz}$  and  $\tau_{yz}$  are the stress tensor components in elastic half-space  $z < 0$ , and  $u_{sz}$  is the component of elastic displacement vector. The “rad” and “ref” indices denote, respectively, waves radiated by a sound source and reflected from plane  $z = 0$  in the acoustic medium. The source term in Eq. (1)<sub>1</sub> for reflected wave may be neglected.

Elastic stress tensor  $\boldsymbol{\sigma}(\mathbf{x}, t)$  and displacement vector  $\mathbf{u}_s(\mathbf{x}, t)$  are expressed by the scalar and vector potentials  $\varphi$  and  $\boldsymbol{\psi}$ , which satisfy the following wave equations (ACHENBACH, 1973):

$$\begin{aligned} \nabla^2 \varphi - \frac{1}{c_L^2} \frac{\partial^2 \varphi}{\partial t^2} &= 0, \\ \nabla^2 \boldsymbol{\psi} - \frac{1}{c_T^2} \frac{\partial^2 \boldsymbol{\psi}}{\partial t^2} &= 0, \quad (\nabla \cdot \boldsymbol{\psi} = 0, \quad \nabla^2 \equiv \nabla \cdot \nabla). \end{aligned}$$

Here,  $c_L = \sqrt{(\lambda + 2\mu) / \rho_s}$  and  $c_T = \sqrt{\mu / \rho_s}$  are the velocities of longitudinal and transversal waves,  $\lambda$  and  $\mu$  are the Lamé elastic parameters while  $\rho_s$  is the material density of solid.

We apply the complex integral Fourier transforms over space variables  $x, y$  and time  $t$  to solve the problem. By solving the problem in Fourier transforms and returning to the originals, as shown before (PIDUBNIAK, PIDUBNIAK, 2010), we obtain:

$$p_{\text{rad}}(\mathbf{x}, t) = \mathbf{F}_0 \cdot \nabla P_{\text{rad}}(\mathbf{x}, t), \quad (2)$$

$$p_{\text{ref}}(\mathbf{x}, t) = \mathbf{F}_0 \cdot \nabla^* P_{\text{ref}}(\mathbf{x}, t), \quad (3)$$

where  $\nabla^* = \nabla_{\perp} - \mathbf{i}_z \partial / \partial z$  and

$$P_{\text{rad}}(\mathbf{x}, t) = -\frac{1}{4\pi} \int_{-\infty}^{\infty} \int_{-\infty}^{\infty} G(a^*) \frac{d\boldsymbol{\xi}'}{R_w(\boldsymbol{\xi}', z - z_0)}, \quad (4)$$

$$P_{\text{ref}}(\mathbf{x}, t) = -\frac{1}{4\pi} \int_{-\infty}^{\infty} \int_{-\infty}^{\infty} G(b^*) \frac{R(\boldsymbol{\xi}', z + z_0) d\boldsymbol{\xi}'}{R_w(\boldsymbol{\xi}', z + z_0)}, \quad (5)$$

where

$$G(a^*) \equiv G\left\{\boldsymbol{\xi} - \boldsymbol{\xi}', t - \frac{1}{c\alpha_{xy}} [R_w(\boldsymbol{\xi}', z - z_0) - \mathbf{M}_w \cdot \boldsymbol{\xi}']\right\},$$

$$G(b^*) \equiv G\left\{\boldsymbol{\xi} - \boldsymbol{\xi}', t - \frac{1}{c\alpha_{xy}} [R_w(\boldsymbol{\xi}', z + z_0) - \mathbf{M}_w \cdot \boldsymbol{\xi}']\right\}.$$

Here,  $\boldsymbol{\xi}' = (x', y')$ ,  $d\boldsymbol{\xi}' = dx' dy'$

$$R_w(\mathbf{x}) = \sqrt{\alpha_y x^2 + \alpha_x y^2 + \beta_{xy} xy + \alpha_{xy} z^2},$$

$$R(\mathbf{x}) = V^-(\mathbf{x})/V^+(\mathbf{x}),$$

$$V^{\pm}(\mathbf{x}) = [S_T^2 - 2S^2(\mathbf{x})]^2 + 4S^2(\mathbf{x})S_{zL}(\mathbf{x})S_{zT}(\mathbf{x})$$

$$\pm N_s S_T^2 (c/c_T)^2 [1 - \mathbf{M}_w \cdot \boldsymbol{\xi}/R_w(\mathbf{x})]^2$$

$$\times S_{zL}(\mathbf{x})/S_z(\mathbf{x}),$$

$$S(\mathbf{x}) = |\mathbf{S}(\mathbf{x})|,$$

$$\mathbf{S}(\mathbf{x}) = \mathbf{r}(\boldsymbol{\xi})/R_w(\mathbf{x}) - \mathbf{M}_w,$$

$$\mathbf{r}(\boldsymbol{\xi}) = (\alpha_y x + \beta_{xy} y, \beta_{xy} x + \alpha_x y),$$

$$S_{zA}(\mathbf{x}) = \sqrt{S_A^2 - S^2(\mathbf{x})},$$

$$S_A = \alpha_{xy} c/c_A \quad (A = L, T),$$

$$S_z(\mathbf{x}) = \alpha_{xy} z/R_w(\mathbf{x}),$$

$$N_s = \rho/\rho_s,$$

$$\mathbf{M}_w = \mathbf{v}_w/c,$$

$$\alpha_x = 1 - M_{wx}^2,$$

$$\alpha_y = 1 - M_{wy}^2,$$

$$\alpha_{xy} = 1 - M_w^2,$$

$$\beta_{xy} = 2M_{wx}M_{wy},$$

$R(\mathbf{x})$  is the reflection coefficient, as the function of angle spherical coordinates and physical-mechanical pa-

rameters of the acoustic and elastic media,  $\mathbf{M}_w$  is the Mach number vector for wind.

It may be noticed that Eq. (4) is exact, but Eq. (5) is found as the inverse of Fourier transformations with the application of the stationary-phase approximation method (FELSEN, MARKUVITZ, 1973). The Eq. (5) does not take into account the small contribution of Rayleigh surface wave in reflected field.

For one-point source radiated harmonic sound wave with circular frequency  $\Omega_0$  and moved with velocity  $v_0$  on height  $z = z_0$  along a line the function  $G(\boldsymbol{\xi}, t)$  may be represented as

$$\begin{aligned} G(\boldsymbol{\xi}, t) &= G_1(\boldsymbol{\xi}, t) \\ &= \delta(x + x_{10} - v_0 t) \delta(y + \xi_0) e^{-i\Omega_0 t} \end{aligned} \quad (6)$$

if source moves along straight line  $-\infty < x < \infty$ ,  $y = -\xi_0$  in positive direction of axis  $Ox$ ;

$$\begin{aligned} G(\boldsymbol{\xi}, t) &= G_2(\boldsymbol{\xi}, t) \\ &= \delta(x - x_{20} + v_0 t) \delta(y - \xi_0) e^{-i\Omega_0 t} \end{aligned} \quad (7)$$

if source moves along straight line  $-\infty < x < \infty$ ,  $y = \xi_0$  in negative direction of axis  $Ox$ ;

$$\begin{aligned} G(\boldsymbol{\xi}, t) &\equiv G^+(\boldsymbol{\xi}, t) \\ &= [G_I^+(\boldsymbol{\xi}, t) + G_{II}^+(\boldsymbol{\xi}, t) + G_{III}^+(\boldsymbol{\xi}, t)] e^{-i\Omega_0 t} \end{aligned} \quad (8)$$

with

$$\begin{aligned} G_I^+(\boldsymbol{\xi}, t) &= \delta(x + x_0 - v_0 t) \delta(y + \xi_0) H(-x), \\ G_{II}^+(\boldsymbol{\xi}, t) &= \delta(x + x_0 - \xi_0) \delta[y - v_0(t - t_1^+)] H(y), \\ G_{III}^+(\boldsymbol{\xi}, t) &= \delta(\xi - \xi_0) \delta[\xi_0(\theta - 3\pi/2) - v_0(t - t_0^+)] \\ &\quad \times [H(2\pi - \theta) - H(3\pi/2 - \theta)] \end{aligned} \quad (9)$$

for source that moves along line with a bend in counter-clockwise order of motion;

$$\begin{aligned} G(\boldsymbol{\xi}, t) &\equiv G^-(\boldsymbol{\xi}, t) \\ &= [G_I^-(\boldsymbol{\xi}, t) + G_{II}^-(\boldsymbol{\xi}, t) + G_{III}^-(\boldsymbol{\xi}, t)] e^{-i\Omega_0 t} \end{aligned} \quad (10)$$

with

$$\begin{aligned} G_{II}^-(\boldsymbol{\xi}, t) &= \delta(x - \xi_0) \delta(y - y_0 + v_0 t) H(y), \\ G_I^-(\boldsymbol{\xi}, t) &= \delta[x + v_0(t - t_1^-)] \delta(y + \xi_0) H(-x), \\ G_{III}^-(\boldsymbol{\xi}, t) &= \delta(\xi - \xi_0) \delta[\xi_0(2\pi - \theta) - v_0(t - t_0^-)] \\ &\quad \times [H(2\pi - \theta) - H(3\pi/2 - \theta)] \end{aligned} \quad (11)$$

for source that moves along line with a bend in clockwise order.

Here  $H(x)$  is the Heaviside function and

$$\begin{aligned} t_0^+ &= x_0/v_0, \\ t_1^+ &= t_0^+ + (\pi/2)\xi_0/v_0 = s^+/v_0, \\ s^+ &= x_0 + (\pi/2)\xi_0, \\ t_0^- &= y_0/v_0, \\ t_1^- &= t_0^- + (\pi/2)\xi_0/v_0 = s^-/v_0, \\ s^- &= y_0 + (\pi/2)\xi_0. \end{aligned} \quad (12)$$

Substituting function  $G(\xi, t)$  from (6)–(11) into integrals (4) and (5) after some transformations we obtained the complex amplitudes of acoustical pressure in the waves radiated from single sources moving along considering routes in two opposite directions, and the waves reflected from the surface of interface of acoustical and elastic media.

Then for the total acoustical pressures we found:

$$p_{\text{tot}}(\mathbf{x}, t, \Omega_0) \equiv [p_{\text{rad}}(\mathbf{x}, t, \Omega_0) + p_{\text{ref}}(\mathbf{x}, t, \Omega_0)]e^{-i\Omega_0 t}, \quad (13)$$

where, respectively,

$$\begin{aligned} p_j(\mathbf{x}, t, \Omega_0) &\equiv p_{j,12}(\mathbf{x}, t, \Omega_0) = p_{j,12}^+(\mathbf{x}, t, \Omega_0) \\ &+ p_{j,12}^-(\mathbf{x}, t, \Omega_0), \quad (j = \text{rad, ref}) \end{aligned} \quad (14)$$

are solutions for the case of travelling along straight lines (Fig. 2a) and

$$\begin{aligned} p_j(\mathbf{x}, t, \Omega_0) &\equiv p_j^\pm(\mathbf{x}, t, \Omega_0) \\ &= \sum_{S=I}^{III} p_{j,S}^\pm(\mathbf{x}, t, \Omega_0), \quad (j = \text{rad, ref}) \end{aligned} \quad (15)$$

are solutions for the case of travelling along routes with a road bend (Fig. 2b, c) with functions  $p_{j,12}^\pm(\mathbf{x}, t, \Omega_0)$  and  $p_{j,S}^\pm(\mathbf{x}, t, \Omega_0)$  ( $S = I, II, III$ ;  $j = \text{rad, ref}$ ) presented in Appendix.

In the case with many sources travelling along mentioned above road lanes the summation of correspondent expressions for complex amplitude of acoustical pressure was carried out.

Thus, for the routes 1–2 we have (Fig. 2a)

$$\begin{aligned} p_{\text{tot},12}(\mathbf{x}, t) &= \sum_{A=L,C} \left[ \sum_{j=0}^{N_{A1}} p_{\text{tot},12}^+(x+x_{10}+j\Delta_A-vAt, \right. \\ &\quad \left. y+\xi_0, z, h_A, \Omega_A) \right. \\ &+ \sum_{j=0}^{N_{A2}} p_{\text{tot},12}^-(x-x_{20}-j\Delta_A+vAt, \\ &\quad \left. y-\xi_0, z, h_A, \Omega_A) \right]. \end{aligned} \quad (16)$$

Similarly, for the case of routes shown in the Fig. 2 b,c, respectively, we obtain:

$$\begin{aligned} p_{\text{tot}}^+(\mathbf{x}, t) &= \sum_{A=L,C} \sum_{j=0}^{N_A^+} \left\{ p_{\text{tot},I}^+(x+x_{A0}+j\Delta_A-vAt, \right. \\ &\quad \left. y+\xi_0, z, h_A, \Omega_A) \right. \\ &+ p_{\text{tot},II}^+[x-\xi_0, y+s_{A_j}^+(t), z, h_A, \Omega_A] \\ &+ p_{\text{tot},III}^+[x-\xi_0 \cos \theta_{A_j}^+(t), \\ &\quad \left. y-\xi_0 \sin \theta_{A_j}^+(t), z, h_A, \Omega_A) \right\}, \end{aligned} \quad (17)$$

$$\begin{aligned} p_{\text{tot}}^-(\mathbf{x}, t) &= \sum_{A=L,C} \sum_{j=0}^{N_A^-} \left\{ p_{\text{tot},II}^-(x-\xi_0, y-y_{A0} \right. \\ &\quad \left. -j\Delta_A+vAt, z, h_A, \Omega_A) \right. \\ &+ p_{\text{tot},I}^-[x-s_{A_j}^-(t), y+\xi_0, z, h_A, \Omega_A] \\ &+ p_{\text{tot},III}^-[x-\xi_0 \cos \theta_{A_j}^-(t), \\ &\quad \left. y-\xi_0 \sin \theta_{A_j}^-(t), z, h_A, \Omega_A) \right\}, \end{aligned} \quad (18)$$

where

$$\begin{aligned} s_{A_j}^+(t) &= x_{0A} + j\Delta_A - vAt + (\pi/2)\xi_0, \\ s_{A_j}^-(t) &= y_{0A} + j\Delta_A - vAt + (\pi/2)\xi_0, \\ \theta_{A_j}^+(t) &= 3\pi/2 + (vAt - x_{0A} - j\Delta_A)/\xi_0, \\ \theta_{A_j}^-(t) &= 2\pi - (v_{0A}t - y_{0A} - j\Delta_A)/\xi_0. \end{aligned} \quad (19)$$

In Eqs. (16)–(18)  $N_{A1}, N_{A2}, N_A^+, N_A^-$  are the numbers of sources,  $\Delta_A$  are the distances between them,  $x_{A0}, y_{A0}$  are the initial source locations in moment  $t = 0$  ( $A = L, C$ ). It was noted that in the formulae (34) components of mass load vectors  $F_{0x}, F_{0y}, F_{0z}, F_{0\xi}, F_{0\theta}$  are replaced with  $F_{Ax}, F_{Ay}, F_{Az}, F_{A\xi}, F_{A\theta}$  ( $A = L, C$ ).

Having the solutions of particular problems for the cases of straight and of curve lines, we may construct the solution to our general problem. However, each particular task was analyzed in their different systems of coordinates. Therefore, it was necessary to attach the local coordinate systems, added to appropriate lines of roads, to general system of coordinates  $Oxy$  represented in Fig. 1. Figure 3a shows the road with straight lines 1–2.

Next, Figs. 3b and 3c illustrate the lines of motion 4–5 and 3–6, respectively, with their local coordinate systems, denoted by subscripts. Here, the coordinates with prime symbol correspond to local systems of coordinates, as on Figs. 2b, c, and without this sign –

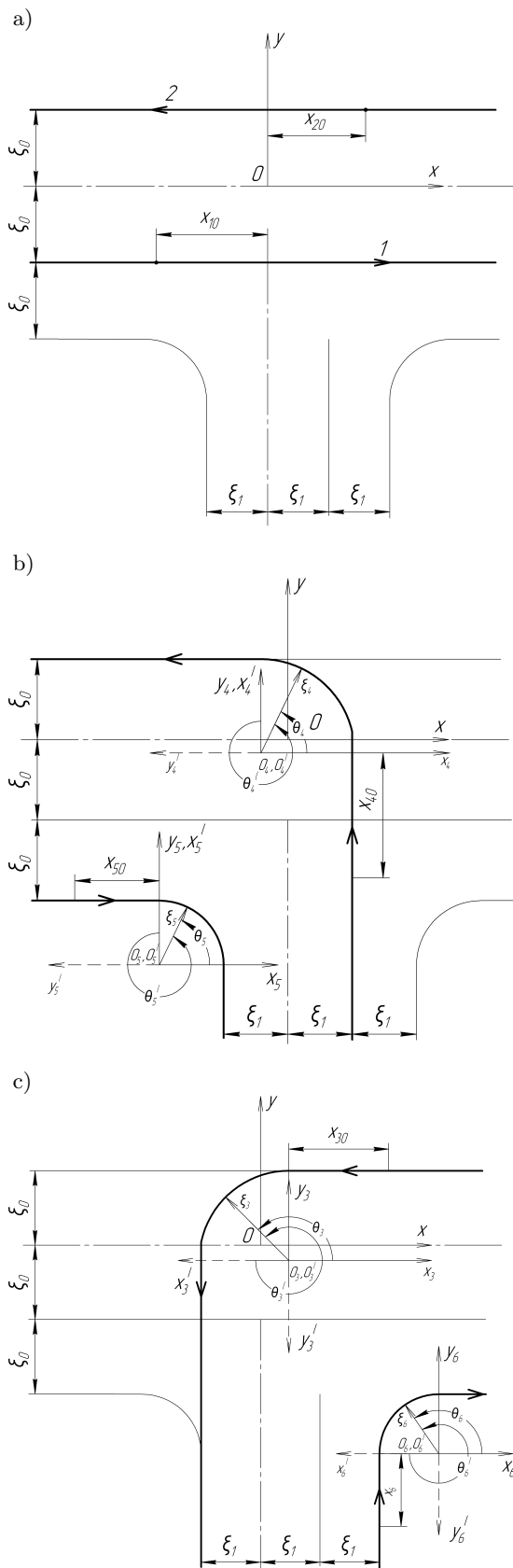


Fig. 3. Scheme of roads with the local systems of Cartesian and polar coordinates: a) lines of straight motion 1 and 2; b) lines of motion on right-angle bend 4 and 5; c) lines of motion on right-angle bend 3 and 6.

to systems oriented on system  $Oxy$ . Thus, from these figures we obtained the following relations:

$$\begin{aligned}
 x'_4 &= y_4 = y + \xi_0 - \xi_4, \\
 y'_4 &= -x_4 = -(x - \xi_1 + \xi_4), \\
 x'_5 &= y_5 = y + 2\xi_0 + \xi_5, \\
 y'_5 &= -x_5 = -(x + \xi_1 + \xi_5), \\
 x'_3 &= -x_3 = -(x + \xi_1 - \xi_3), \\
 y'_3 &= -y_3 = -(y - \xi_0 + \xi_3), \\
 x'_6 &= -x_6 = -(x - 2\xi_1 - \xi_6), \\
 y'_6 &= -y_6 = -(y + 2\xi_0 + \xi_6),
 \end{aligned}
 \tag{20}$$

where  $\xi_0$  is the line distance of motion from main road axis,  $\xi_1$  is the line distance of motion from axis of minor road perpendicular to main road,  $\xi_j$  ( $j = 3, 4, 5, 6$ ) are the radii of bend of appropriated lines of motion.

For determination of complex amplitudes of acoustic pressure in the case of sound sources on routes 3, 4, 5 and 6 (Fig. 3b, c) the variables  $x'_j, y'_j$  ( $j = 3, 4, 5, 6$ ) from Eqs. (20) were substituted to corresponding functions in the Eqs. (17), (18) instead of variables  $x$  and  $y$ . It means that for the routes 3 and 4 we used the functions from Eq. (17), and for the routes 5 and 6 – the functions from Eq. (18).

For determination of the acoustic field on cross-road displayed in Fig. 1 we presumed that motion occurs periodically during time period  $t_0 = t_{12} + t_{45} + t_{36}$ , where  $t_{12}, t_{45}, t_{36}$  are, respectively, the during times of motion along lanes 1–2, 4–5, 3–6. Then for total acoustical pressure the following expression was obtained:

$$\begin{aligned}
 p_{\text{tot}}(\mathbf{x}, t) &= \sum_{m=1}^M \{ p_{\text{tot},12}(\mathbf{x}, t_{1m}) H(t_{1m}) \\
 &+ [p_{\text{tot},4}(\mathbf{x}, t_{2m}) + p_{\text{tot},5}(\mathbf{x}, t_{2m})] H(t_{2m}) \\
 &+ [p_{\text{tot},3}(\mathbf{x}, t_{3m}) + p_{\text{tot},6}(\mathbf{x}, t_{3m})] H(t_{3m}) \},
 \end{aligned}
 \tag{21}$$

where  $t_{1m} = t - (m - 1)t_0$ ,  $t_{2m} = t - (m - 1)t_0 - t_{12}$ ,  $t_{3m} = t - (m - 1)t_0 - t_{12} - t_{45}$  ( $m = 1, 2, \dots, M$ ),  $M$  is the number accounted periods. In the Eqs. (21), (17) and (18) the numbers  $N_A^+$  were changed on  $N_{A3}$  and  $N_{A4}$  for vehicles on lanes 3 and 4, and number  $N_A^-$  was changed on  $N_{A5}$  and  $N_{A6}$  for vehicles on lanes 5 and 6 ( $A = L, C$ ).

Using Eq. (21) the instantaneous acoustic pressure level from the considered sources of noise (in dB or phones) was determined

$$L_p(\mathbf{x}, t) = 20 \log_{10} \left( \frac{|p_{\text{tot}}(\mathbf{x}, t)|}{p_0} \right),
 \tag{22}$$

where  $p_0 = 2 \cdot 10^{-5}$  Pa is the threshold pressure.

The other energetic characteristic used as a result of noise analysis is the acoustic pressure level averaged over some time period  $T_0$  (MÜLLER, MÖSER, 2013)

$$L_{p,av}(\mathbf{x}) = 10 \log_{10} \left\{ \frac{1}{T_0} \int_{t_*}^{t_*+T_0} \left[ \frac{|p_{tot}(\mathbf{x}, t)|}{p_0} \right]^2 dt \right\} \quad (t_* \geq 0). \quad (23)$$

### 3. Numerical analysis of the acoustic field from vehicles as an example of the city roads T junction

For numerical analysis we take  $F_{Ax} = F_{Ay} = F_{Az} = F_{A\xi} = F_{A\theta} = F_A$  ( $A = L, C$ ). It can be shown that  $F_A K_A \approx 4\pi \cdot 10^{L_{p,A}/20} p_0 \cdot 1$  metre, where  $L_{p,A}$  is the average acoustical pressure level measured at one-metre distance from unmoved individual sound source of  $A$ -type,  $K_A = \Omega_A/c$  ( $A = L, C$ ). Then for numerical calculations we also take  $L_{p,L} = 75$  dB for passenger cars and  $L_{p,C} = 85$  dB for trucks (ENGEL, 2001). Similarly, the frequencies of source vibrations are  $\Omega_L = 300$  Hz and  $\Omega_C = 250$  Hz. The motor vehicles move in air medium with density  $\rho = 1.293$  kg/m<sup>3</sup> and sound speed  $c = 331$  m/s. The road is coated by asphalt with material density  $\rho_s = 2000$  kg/m<sup>3</sup> and velocities of longitudinal and transversal waves  $c_L = 3468$  m/s,  $c_T = 1667$  m/s (KETTIL *et al.*, 2005). The heights of sources are  $h_L = 1$  m and  $h_C = 2$  m.

As model situation we considered a typical T junction of Wólczajska and Wróblewskiego streets in Łódź (Poland) taking into consideration the wind influence. The distances of motion lanes from road axes were  $\xi_0 = \xi_1 = 5$  m, and the radii of bend were  $\xi_3 = \xi_4 = 7$  m,  $\xi_5 = \xi_6 = 20$  m. From 1 to 2 pm on October 23rd, 2012 it was observed that 1956 passenger cars and 66 trucks passed in different directions<sup>1</sup>. On average within 120 s we obtained:  $N_{L1} = 11, N_{L2} = 15, N_{L3} = 13, N_{L4} = 6, N_{L5} = 7, N_{L6} = 13, N_{Cn} = 1$  ( $n = \overline{1, 6}$ ). Assuming approximately that on the small area within a cross-road the vehicles velocities were identical and equal  $v_L = v_C = 40$  km/h, we found the following parameters  $\Delta_{Ln} = 40$  m,  $\Delta_{Cn} = 1000$  m ( $n = \overline{1, 6}$ ). For this time the average 13 passenger cars (or 40%) passed on routes 1–2 and 3–6, and also 7 (20%) passed on routes 4–5. In such conditions we divided the times of passing across this part of road for 120 s in following rations:  $t_{12} = t_{36} = 50$  s and  $t_{45} = 20$  s. The calculations were mainly done for height  $z = 4$  m.

The total acoustic pressure  $Re(p_{tot})$  (in Pa) is displayed in Figs. 4a, b, c, d as function of time for windless conditions on the ray goes out from the origin of coordinates  $Oxy$  with  $\theta = 315^\circ$ . The numerical calcu-

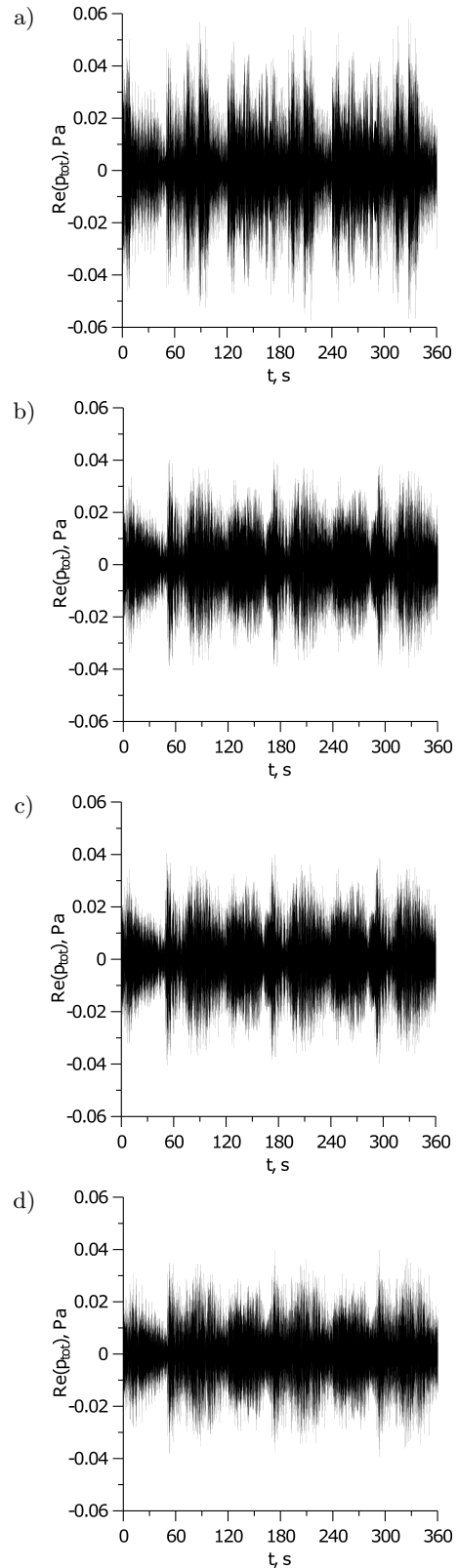


Fig. 4. Acoustic pressure  $Re(p_{tot})$  as time variable function in windless conditions calculated in different points of observation: a) in center of road bend:  $x = -25, y = -30$ ; b) on the axis of this bend:  $x = -39.4, y = -44.4$ ; c)  $x = -53.3, y = -58.3$ ; d)  $x = -67.4, y = -72.4$  (in meters).

<sup>1</sup>The observations were done by student of Lodz University of Technology Oleksandr Krasnyk.

lations were done in four points on axis of symmetry of 5th road lane:

- a)  $x = -[\xi_1 + \xi_5(1 - \sqrt{2})] \approx -10.9$  m,  
 $y = -[2\xi_0 + \xi_5(1 - \sqrt{2})] \approx -15.9$  m,
- b)  $x = -(\xi_1 + \xi_5) = -25$  m,  
 $y = -(2\xi_0 + \xi_5) = -30$  m,
- c)  $x = -[\xi_1 + \xi_5(1 + \sqrt{2})] \approx -29.1$  m,  
 $y = -[2\xi_0 + \xi_5(1 + \sqrt{2})] \approx -44.1$  m

during 360 s (i.e. for three time periods,  $M = 3$ ) for each case. In consequence of different frequencies  $\Omega_L$  and  $\Omega_C$  of sound radiation from acoustic sources and non-symmetric conditions of cars motion the total wave field is incoherent and structure of acoustic pressure pulses in these points of observation is complicated. The signal of acoustic pressure is presented by superposition of short quasi-monochromatic wave packets, the amplitude of which decreases with distance from source as a result of geometric divergence of sound waves. The great amplitudes in Fig. 4a correspond to signals radiated from trucks, number of which at this time is small. Therefore, in general case the signals were formed by passenger cars.

In Fig. 5 the influence of wind velocity ( $v_w = 20, 40$  and  $60$  km/h;  $\theta_w = 180^\circ$ ) on structure acoustical pressure is illustrated. The signals were calculated on distance 40 m from the bend of road ( $x = -y = 192$  m). These graphs illustrate the signal ‘diffusion’ and decreasing in such way of acoustic pressure amplitude caused by increasing wind velocity. Similar effects were noted in the structure of signals radiated by vehicles on roundabout (PIDDUBNIAK, PIDDUBNIAK, 2010). Thus, the influence of wind parameters on the radiated signal is evident.

The effect of wind direction on the structure of acoustic signals is shown in Figs. 6 and 7. There, the value of  $\text{Re}(p_{\text{tot}})$  was calculated also at distance of 40 m from the axis of road bend ( $x = -y = 192$  m) as a function of time with wind velocity ( $v_w = 40$  km/h) for four mutually opposite wind directions, namely,  $\theta_w = 0^\circ$  and  $180^\circ$ ,  $45^\circ$  and  $225^\circ$ ,  $90^\circ$  and  $270^\circ$ ,  $135^\circ$  and  $315^\circ$ .

Thus, the changes in the Doppler effect, caused by the presence of wind, substantially affect inner structure of observed sound pulses.

Figure 8 displays the space distribution of acoustic pressure level  $L_p(x, y) \equiv L_p(x, y, 0)$  (in dB), calculated on the basis of Eqs. (21) and (22). The calculations were carried out in windy conditions ( $v_w = 40$  km/h,  $\theta_w = 315^\circ$ ). As it is shown in this case, sound propagation is characterized by a high acoustic pressure level (over 75 dB) over straight road and curved road section and considerable reduction (near 50–60 dB) on the same distance of 40–60 m from road.

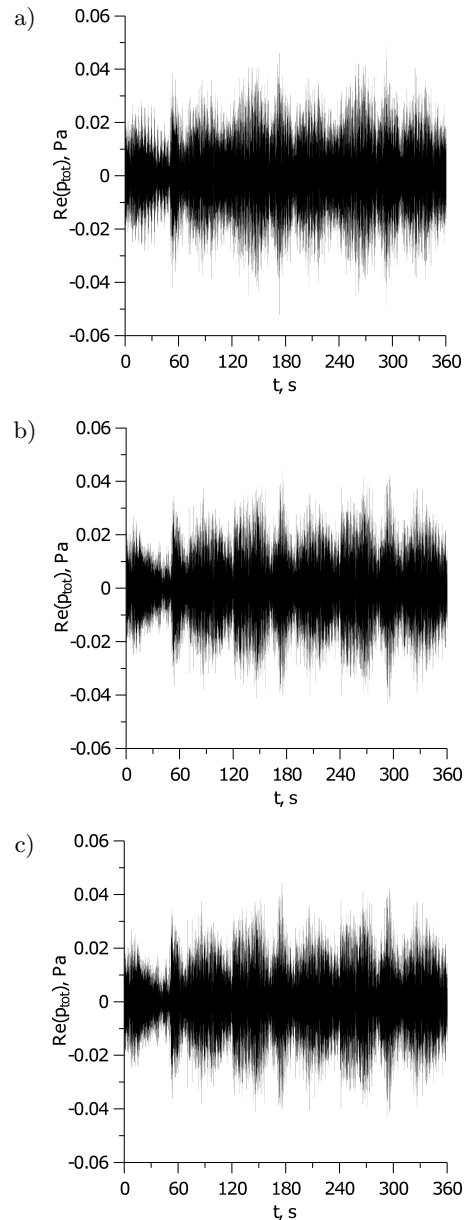


Fig. 5. Acoustic pressure  $\text{Re}(p_{\text{tot}})$  as time variable function calculated on distance 40 m from the right bend of road ( $x = -y = 192$  m) with taking into consideration wind velocity ( $\theta_w = 180^\circ$ ): a)  $v_w = 20$  km/h; b)  $v_w = 40$  km/h; c)  $v_w = 60$  km/h.

Figures 9–11 show the space distribution of acoustic sound level  $L_{p,\text{av}}(\mathbf{x})$  (in dB) averaged over time period  $T_0 = t_0 = 120$  s. The calculations were obtained with Eqs. (21) and (23) ( $t_* = 0$ ) in the plane  $Oxy$  on the heights 4, 8 and 12 m but neglecting the wind effect. It may be noted that T junction of city roads is the place of high noise concentration (near 80 dB), which amplitude gradually decreases with increasing of distance from this road element. In particular, on distance of 100 m from the center of T intersection the averaged acoustic pressure level decreases almost to 55 dB.



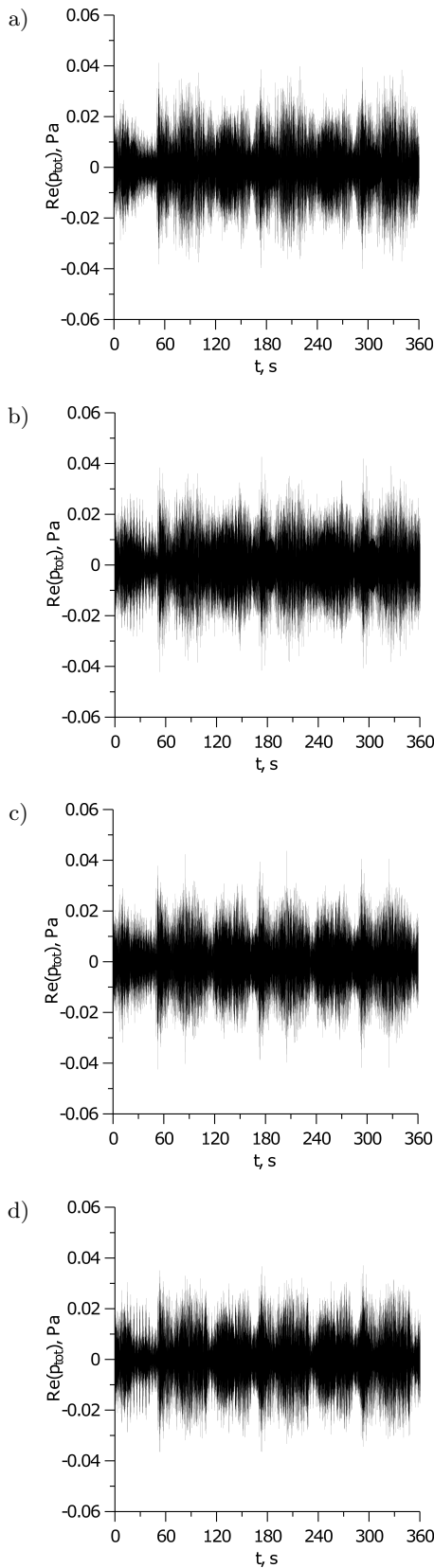


Fig. 6. Acoustic pressure  $\text{Re}(p_{\text{tot}})$  at the distance of 40 m from the road bend ( $x = -y = 192$  m) vs. time taking wind direction into consideration ( $v_w = 40$  km/h): a)  $\theta_w = 0^\circ$ ; b)  $\theta_w = 180^\circ$ ; c)  $\theta_w = 45^\circ$ ; d)  $\theta_w = 225^\circ$ .

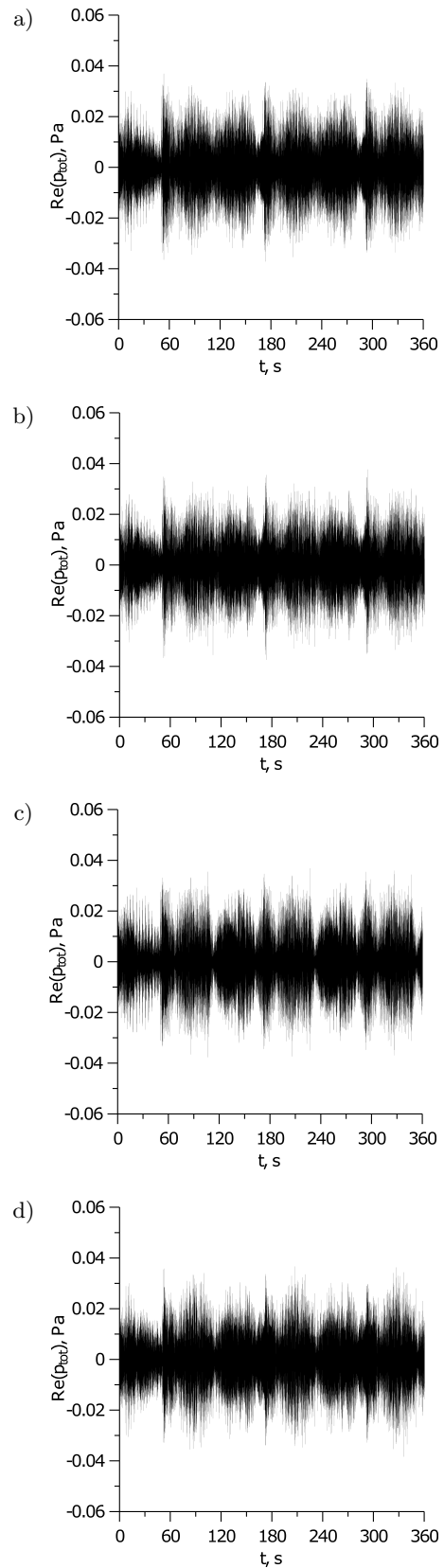


Fig. 7. Acoustic pressure  $\text{Re}(p_{\text{tot}})$  at the distance of 40 m from the road bend ( $x = -y = 192$  m) vs. time taking wind direction into consideration ( $v_w = 40$  km/h): a)  $\theta_w = 90^\circ$ ; b)  $\theta_w = 270^\circ$ ; c)  $\theta_w = 135^\circ$ ; d)  $\theta_w = 315^\circ$ .

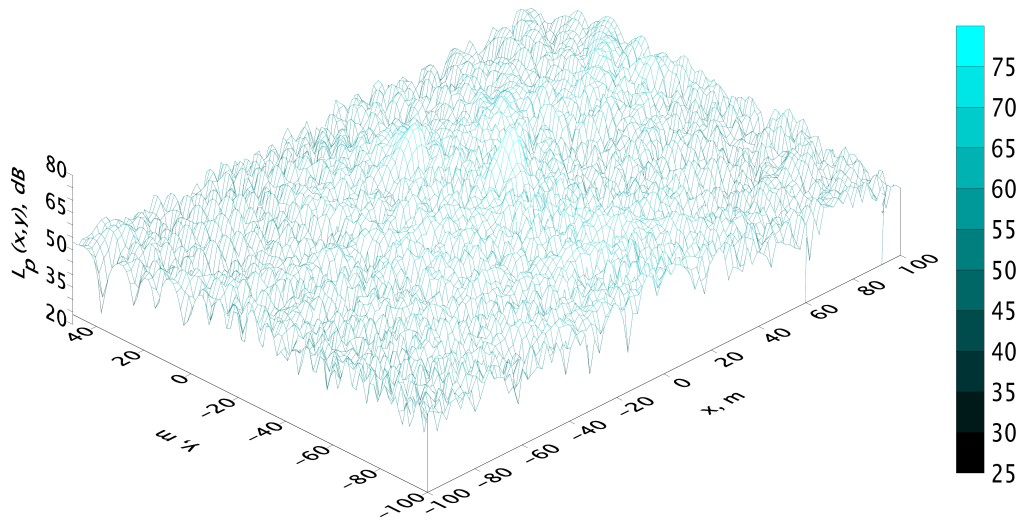


Fig. 8. Acoustic sound level distribution in space  $L_p(x,y)$  in the moment of time  $t = 11$  s on the square  $200 \times 150$  m,  $z = 4$  m for  $v_w = 30$  km/h and  $\theta_w = 315^\circ$ .

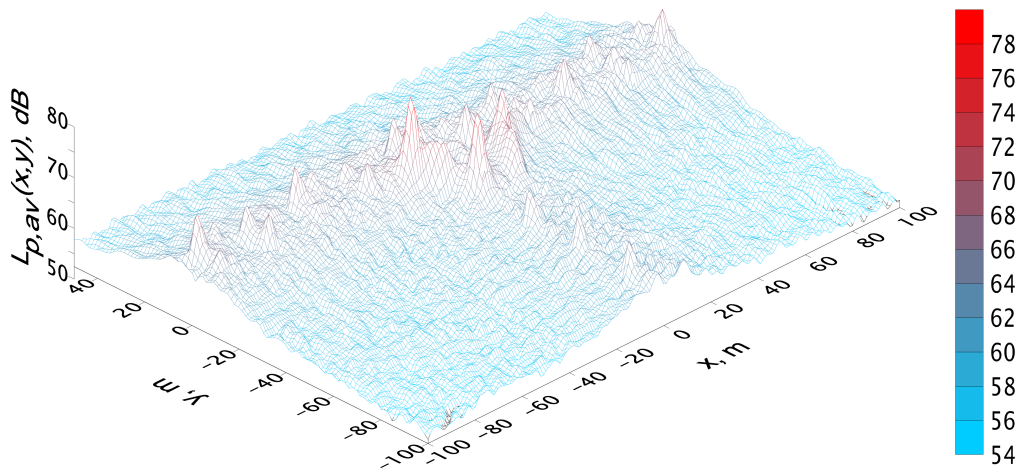


Fig. 9. Average sound intensity distribution  $L_{p,av}(x,y)$  on the area  $x \times y = 200 \times 150$  m,  $z = 4$  m in windless conditions.

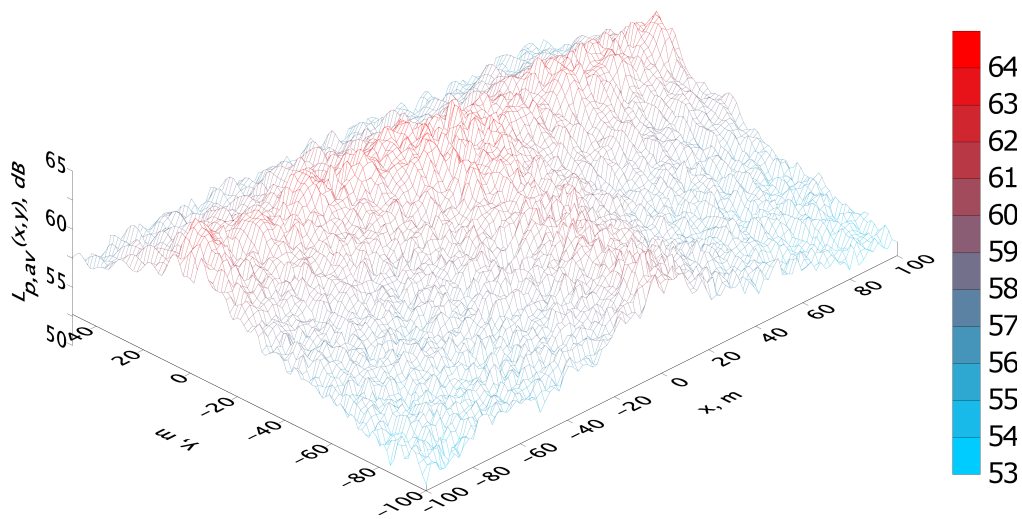


Fig. 10. Average sound intensity distribution  $L_{p,av}(x,y)$  on the area  $x \times y = 200 \times 150$  m,  $z = 8$  m in windless conditions.

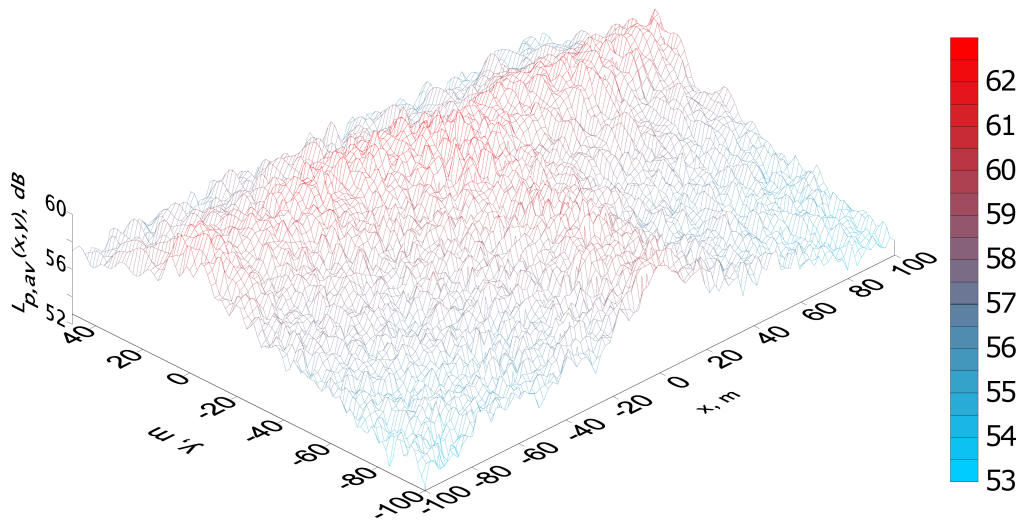


Fig. 11. Average sound intensity distribution  $L_{p,av}(x,y)$  on the area  $x \times y = 200 \times 150$  m,  $z = 12$  m in windless conditions.

### 4. Conclusions

In this work the analytical-numerical approach to the description of vehicle sound radiation from a T junction of city roads taking into consideration wave reflection from the boundary interface: acoustic moving media – elastic half-space and wind conditions was developed. The solution of problem was obtained with the help of Fourier transforms over time and space variables, and using the stationary phase method. The general solution in this problem was found as superposition of the solutions for the cases of road elements in the forms of straight lines and lines with a bend. The mathematical modelling was carried out for a dual carriageway road with one lane each in opposite directions for passengers' cars and heavy trucks. For mathematical simulation data collected from one of Lodz streets were used. The main numerical results of this work are as follows:

1. The acoustic signal from many vehicles as monopole sound sources moving on the T junction of city road is presented as a complicated superposition of two series of quasi-monochromatic sinusoidal pulses (with Doppler effect influence; see: Appendix). The calculations carried out in the immediate proximity to the road show acoustical pressure amplitudes decreasing from 0.08 to 0.05 Pa in limits of 40 m.
2. The straight and curved road sections are the places of high concentration of sound energy, where the acoustic pressure level can increase by 20–30 dB in comparison to the outside of road (Figs. 8–11).
3. The velocity (in a limits of 20 do 60 km/h) and direction of wind influenced considerably the acoustical pressure and acoustical pressure level near

road mainly on inner structure of these characteristic, but not for amplitude (Figs. 5–7).

4. The analysis shows that maximal values of the average acoustical pressure level weakened from 80 dB to 63 dB on the height 4–12 m over road (Figs. 9–11).
5. The offered mathematical modelling shows that this element of road with travelling vehicles can be interpreted as linear acoustic antenna in the form of letter *T*.
6. The analytical and numerical approach offered in this article can extend possibilities of empiric and technical acoustic models for estimation of traffic noise level on existing and designed roads with different complex geometry.

### Appendix

Substituting function  $G(\xi, t)$  from (6)–(11) into integrals (4) and (5), and applying the property of Dirac function (KECS, TEODORESCU, 1978):

$$\delta[f(x)] = \sum_j \frac{\delta(x - x_j)}{|f'(x_j)|}, \tag{24}$$

where  $x_j$  are zeros of  $f(x)$ ,  $f'(x_j)$  is the derivative of  $f(x)$  over  $x$  in point  $x = x_j$ , as well as the property of

$$\int_a^b f(y)\delta(x - y) dy = f(x)[H(x - a) - H(x - b)], \tag{25}$$

we calculated acoustic potentials in radiated and reflected waves  $P_{rad}(\mathbf{x}, t)$  and  $P_{ref}(\mathbf{x}, t)$ :

$$P_j(\mathbf{x}, t) \equiv P_j(\mathbf{x}, t, \Omega_0)e^{-i\Omega_0 t}, \quad (j = rad, ref). \tag{26}$$

Here in the case of travelling along straight routes 1–2 (Fig. 3a) we have (PIDUBNIAK *et al.*, 2009b):

$$\begin{aligned} P_j(\mathbf{x}, t, \Omega_0) &\equiv P_{j,12}(\mathbf{x}, t, \Omega_0) \\ &= P_{j,12}^+(\mathbf{x}, t, \Omega_0) + P_{j,12}^-(\mathbf{x}, t, \Omega_0), \\ &\quad (j = \text{rad}, \text{ref}), \end{aligned} \quad (27)$$

where

$$\begin{aligned} P_{\text{rad},12}^+(\mathbf{x}, t, \Omega_0) &= \\ &= \frac{1}{4\pi R_w^+(x+x_{10}-v_0t, y+\xi_0, z-z_0)} \\ &\times \exp[iK^+L^+(x+x_{10}-v_0t, y+\xi_0, z-z_0)], \\ P_{\text{ref},12}^+(\mathbf{x}, t, \Omega_0) &= \\ &= \frac{R[x+x_{10}-v_0t, y+\xi_0, z+z_0]}{4\pi R_w^+(x+x_0-v_0t, y+\xi_0, z+z_0)} \\ &\times \exp[iK^+L^+(x+x_{10}-v_0t, y+\xi_0, z+z_0)], \end{aligned} \quad (28)$$

$$\begin{aligned} P_{\text{rad},12}^-(\mathbf{x}, t, \Omega_0) &= \\ &= \frac{1}{4\pi R_w^-(x-x_{20}+v_0t, y-\xi_0, z-z_0)} \\ &\times \exp[iK^-L^-(x-x_{20}+v_0t, y-\xi_0, z-z_0)], \\ P_{\text{ref},12}^-(\mathbf{x}, t, \Omega_0) &= \\ &= \frac{R[x-x_{20}+v_0t, y-\xi_0, z+z_0]}{4\pi R_w^-(x-x_{20}+v_0t, y-\xi_0, z+z_0)} \\ &\times \exp[iK^-L^-(x-x_{20}+v_0t, y-\xi_0, z+z_0)] \end{aligned}$$

with

$$\begin{aligned} R_w^\pm(\mathbf{x}) &= \sqrt{\alpha_y x^2 + \alpha_x^\pm y^2 + 2\beta_{xy}^\pm xy + \alpha_{xy}^\pm z^2}, \\ L^\pm(\mathbf{x}) &= R_w^\pm(\mathbf{x}) - M_{wx}^\pm x - M_{wy}^\pm y, \\ \alpha_x^\pm &= 1 - (M_{wx}^\pm)^2, \quad \alpha_y = 1 - M_{wy}^2, \\ \beta_{xy}^\pm &= M_{wx}^\pm M_{wy}, \\ \alpha_{xy}^\pm &= 1 - (M_{wx}^\pm)^2 - M_{wy}^2, \\ M_{wx}^\pm &= M_{wx} \mp M_0, \quad M_0 = v_0/c, \\ K^\pm &= K_0/\alpha_{xy}^\pm, \quad K_0 = \Omega_0/c. \end{aligned} \quad (29)$$

In the case of travelling along routes with a road bend shown in Fig. 3b and Fig. 3c we obtained (PIDUBNIAK *et al.*, 2012):

$$\begin{aligned} P_j(\mathbf{x}, t, \Omega_0) &\equiv P_j^\pm(\mathbf{x}, t, \Omega_0) = \sum_{S=I}^{III} P_{j,S}^\pm(\mathbf{x}, t, \Omega_0), \\ &\quad (j = \text{rad}, \text{ref}), \end{aligned} \quad (30)$$

where

$$\begin{aligned} P_{\text{rad},I}^+(\mathbf{x}, t, \Omega_0) &= -\frac{1}{4\pi R_{w,I}^+(x+x_0-v_0t, y+\xi_0, z-z_0)} \\ &\times \exp[iK_{0,I}^+L_I^+(x+x_0-v_0t, y+\xi_0, z-z_0)] \\ &\times H[x_0-v_0t \\ &+ \varepsilon_I^+L_I^+(x+x_0-v_0t, y+\xi_0, z-z_0)], \\ P_{\text{ref},I}^+(\mathbf{x}, t, \Omega_0) &= -\frac{1}{4\pi R_{w,I}^+(x+x_0-v_0t, y+\xi_0, z+z_0)} \\ &\times R[x+x_0-v_0t+\varepsilon_I^+L_I^+(x+x_0-v_0t, y+\xi_0, \\ &\quad z+z_0), y+\xi_0, z+z_0] \\ &\times \exp[iK_I^+L_I^+(x+x_0-v_0t, y+\xi_0, z+z_0)] \\ &\times H[x_0-v_0t \\ &+ \varepsilon_I^+L_I^+(x+x_0-v_0t, y+\xi_0, z+z_0)], \\ P_{\text{rad},II}^+(\mathbf{x}, t, \Omega_0) &= -\frac{1}{4\pi R_{w,II}^+(x-\xi_0, y+s^+-v_0t, z-z_0)} \\ &\times \exp[iK_{0,II}^+L_{II}^+(x-\xi_0, y+s^+-v_0t, z-z_0)] \\ &\times H[-(s^+-v_0t) \\ &- \varepsilon_{II}^+L_{II}^+(x-\xi_0, y+s^+-v_0t, z-z_0)], \\ P_{\text{ref},II}^+(\mathbf{x}, t, \Omega_0) &= -\frac{1}{4\pi R_{w,II}^+(x-\xi_0, y+s^+-v_0t, z+z_0)} \\ &\times R[x-\xi_0, y+s^+-v_0t+\varepsilon_{II}^+L_{II}^+(x-\xi_0, y \\ &\quad +s^+-v_0t, z+z_0), z+z_0] \\ &\times \exp[iK_{0,II}^+L_{II}^+(x-\xi_0, y+s^+-v_0t, z+z_0)] \\ &\times H[-(s^+-v_0t) \\ &- \varepsilon_{II}^+L_{II}^+(x-\xi_0, y+s^+-v_0t, z+z_0)], \end{aligned} \quad (31)$$

$$\begin{aligned} P_{\text{rad},III}^+(\mathbf{x}, t, \Omega_0) &= -\frac{1}{4\pi R_{w,III}^+(\boldsymbol{\xi}, z-z_0, t)} \\ &\times \exp[iK_{0,III}^+L_{III}^+(\boldsymbol{\xi}, z-z_0, t)] \\ &\times \{H[2\pi-\theta_1^+(\boldsymbol{\xi}, z-z_0, t)] \\ &- H[3\pi/2-\theta_1^+(\boldsymbol{\xi}, z-z_0, t)]\}, \end{aligned}$$

$$\begin{aligned} P_{\text{ref},III}^+(\mathbf{x}, t, \Omega_0) &= -\frac{R^+(\boldsymbol{\xi}, z+z_0, t)}{4\pi R_{w,III}^+(\boldsymbol{\xi}, z+z_0, t)} \\ &\times \exp[iK_{0,III}^+L_{III}^+(\boldsymbol{\xi}, z+z_0, t)] \\ &\times \{H[2\pi-\theta_1^+(\boldsymbol{\xi}, z+z_0, t)] \\ &- H[3\pi/2-\theta_1^+(\boldsymbol{\xi}, z+z_0, t)]\}, \end{aligned}$$

$$\begin{aligned} P_{\text{rad},II}^-(\mathbf{x}, t, \Omega_0) &= -\frac{1}{4\pi R_{w,II}^-(x-\xi_0, y-y_0+v_0t, z-z_0)} \\ &\times \exp[iK_{0,II}^-L_{II}^-(x-\xi_0, y-y_0+v_0t, z-z_0)] \\ &\times H[y_0-v_0t+\varepsilon_{II}^-L_{II}^-(x-\xi_0, y-y_0+v_0t, z-z_0)], \end{aligned}$$

$$\begin{aligned}
 P_{\text{ref},II}^-(\mathbf{x}, t, \Omega_0) &= -\frac{1}{4\pi R_{w,II}^-} \times R[x-\xi_0, y-y_0+v_0t \\
 &\quad - \varepsilon_{II}^- L_{II}^-(x-\xi_0, y-y_0+v_0t, z+z_0), z+z_0] \\
 &\quad \times \exp[iK_{II}^- L_{II}^-(x-\xi_0, y-y_0+v_0t, z+z_0)] \\
 &\quad \times H[y_0-v_0t+\varepsilon_{II}^- L_{II}^-(x-\xi_0, y-y_0+v_0t, z+z_0)], \\
 P_{\text{rad},I}^-(\mathbf{x}, t, \Omega_0) &= -\frac{1}{4\pi R_{w,I}^-} \times \exp[iK_{0,I}^- L_I^-(x-s^-+v_0t, y+\xi_0, z-z_0)] \\
 &\quad \times H[-(s^- - v_0t) \\
 &\quad - \varepsilon_I^- L_I^-(x-s^-+v_0t, y+\xi_0, z-z_0)], \\
 P_{\text{ref},I}^-(\mathbf{x}, t, \Omega_0) &= -\frac{1}{4\pi R_{w,I}^-} \times R[x-s^-, y_0t \\
 &\quad - \varepsilon_I^- L_I^-(x-s^-+v_0t, y+\xi_0, z+z_0), y+\xi_0 z+z_0] \\
 &\quad \times \exp[iK_{0,I}^- L_I^-(x-s^-+v_0t, y+\xi_0, z+z_0)] \\
 &\quad \times H[-(s^- - v_0t) \\
 &\quad - \varepsilon_I^- L_I^-(x-s^-+v_0t, y+\xi_0, z+z_0)], \\
 P_{\text{rad},III}^-(\mathbf{x}, t, \Omega_0) &= -\frac{1}{4\pi R_{w,III}^-} \times \exp[iK_{0,III}^- L_{III}^-(\boldsymbol{\xi}, z-z_0, t)] \\
 &\quad \times \{H[2\pi-\theta_1^-(\boldsymbol{\xi}, z-z_0, t)] \\
 &\quad - H[3\pi/2-\theta_1^-(\boldsymbol{\xi}, z-z_0, t)]\}, \\
 P_{\text{ref},III}^-(\mathbf{x}, t, \Omega_0) &= -\frac{R^-(\boldsymbol{\xi}, z+z_0, t)}{4\pi R_{w,III}^+} \times \exp[iK_{0,III}^- L_{III}^-(\boldsymbol{\xi}, z+z_0, t)] \\
 &\quad \times \{H[2\pi-\theta_1^-(\boldsymbol{\xi}, z+z_0, t)] \\
 &\quad - H[3\pi/2-\theta_1^-(\boldsymbol{\xi}, z+z_0, t)]\} \quad (31)_{\text{Cont.}}
 \end{aligned}$$

with

$$\begin{aligned}
 R_{w,I}^+(\mathbf{x}) &= \sqrt{\alpha_y x^2 + \alpha_{x,I}^+ y^2 + 2\beta_{xy,I}^+ xy + \alpha_{xy,I}^+ z^2}, \\
 R_{w,II}^+(\mathbf{x}) &= \sqrt{\alpha_y x^2 + \alpha_x y^2 + 2\beta_{xy,II}^+ xy + \alpha_{xy,II}^+ z^2}, \\
 R_{w,I}^-(\mathbf{x}) &= \sqrt{\alpha_y x^2 + \alpha_{x,I}^- y^2 + 2\beta_{xy,I}^- xy + \alpha_{xy,I}^- z^2}, \\
 R_{w,II}^-(\mathbf{x}) &= \sqrt{\alpha_y x^2 + \alpha_x y^2 + 2\beta_{xy,II}^- xy + \alpha_{xy,II}^- z^2}, \quad (32)
 \end{aligned}$$

$$\begin{aligned}
 R_{w,III}^\pm(\mathbf{x}, t) &= R_w(\boldsymbol{\xi}-\boldsymbol{\xi}', z) \Big|_{\xi'=\xi_0, \theta'=\theta_0^\pm}, \\
 L_I^+(\mathbf{x}) &= R_{w,I}^+(\mathbf{x}) - M_{wx,I}^+ - M_{wy}y, \\
 L_{II}^+(\mathbf{x}) &= R_{w,II}^+(\mathbf{x}) - M_{wx}x - M_{wy,II}^+ y, \\
 L_I^-(\mathbf{x}) &= R_{w,I}^-(\mathbf{x}) - M_{wx,I}^- - M_{wy}y, \\
 L_{II}^-(\mathbf{x}) &= R_{w,II}^-(\mathbf{x}) - M_{wx}x - M_{wy,II}^- y, \\
 L_{w,III}^\pm(\mathbf{x}, t) &= [R_w(\boldsymbol{\xi}-\boldsymbol{\xi}', z) \\
 &\quad - \mathbf{M}_w \cdot (\boldsymbol{\xi}-\boldsymbol{\xi}')] \Big|_{\xi'=\xi_0, \theta'=\theta_0^\pm(t)}, \\
 \alpha_{x,I}^+ &= 1 - (M_{wx,I}^+)^2, \\
 \beta_{xy,I}^+ &= M_{wx,I}^+ M_{wy}, \\
 \alpha_{xy,I}^+ &= 1 - (M_{wx,I}^+)^2 - M_{wy}^2, \\
 \alpha_{y,II}^+ &= 1 - (M_{wy,II}^+)^2, \\
 \beta_{xy,II}^+ &= M_{wx} M_{wy,II}^+, \\
 \alpha_{xy,II}^+ &= 1 - M_{wx}^2 - (M_{wy,II}^+)^2, \\
 \alpha_{x,I}^- &= 1 - (M_{wx,I}^-)^2, \\
 \beta_{xy,I}^- &= M_{wx,I}^- M_{wy}, \\
 \alpha_{xy,I}^- &= 1 - (M_{wx,I}^-)^2 - M_{wy}^2, \\
 \alpha_{y,II}^- &= 1 - (M_{wy,II}^-)^2, \\
 \beta_{xy,II}^- &= M_{wx} M_{wy,II}^-, \\
 \alpha_{xy,II}^- &= 1 - M_{wx}^2 - (M_{wy,II}^-)^2, \\
 M_{wx,I}^\pm &= M_{wx} \mp M_0, \\
 M_{wy,II}^\pm &= M_{wy} \mp M_0, \\
 K_{0,S}^\pm &= K_0 / \alpha_{xy,S}^\pm, \\
 \varepsilon_S^\pm &= M_0 / \alpha_{xy,S}^\pm \quad (S = I, II), \\
 \varepsilon &= M_0 / \alpha_{xy},
 \end{aligned}$$

$$\begin{aligned}
 \theta_1^\pm(\mathbf{x}, t) &= \theta_0^\pm(t) - (\varepsilon/\xi_0) L_{III}^\pm(\mathbf{x}, t), \\
 \theta_0^+(t) &= 3\pi/2 + (v_0t - x_0)/\xi_0, \\
 \theta_0^-(t) &= 2\pi - (v_0t - y_0)/\xi_0. \quad (32)_{\text{Cont.}}
 \end{aligned}$$

Here the signs “+” and “-”, respectively, correspond to Fig. 2b and Fig. 2c.

Thus, acoustic potentials (26)–(28) and (30), (31) are described by quasi-spherical waves taking into account the reflection waves from the acoustic medium –

elastic half-space interface boundary and the Doppler effect caused by motion of sound sources and acoustic medium (wind).

Substituting functions  $P_{\text{rad}}(\mathbf{x}, \Omega_0, t)$  and  $P_{\text{ref}}(\mathbf{x}, \Omega_0, t)$  from Eqs. (26)–(28) and (30), (31) to Eqs. (2) and (3) we obtained the complex amplitudes of acoustical pressure in the waves radiated from single sources moving along considering routes in two opposite directions, and the waves reflected from the surface of interface of acoustical and elastic media (13)–(15), where

$$\begin{aligned}
p_{\text{rad},12}^+(\mathbf{x}, t, \Omega_0) &= iK_0 \mathbf{F}_0^+ \\
&\cdot \mathbf{A}_{\text{rad},12}^+(x + x_{10} - v_0 t, y + \xi_0, z - z_0) \\
&\times P_{\text{rad},12}^+(\mathbf{x}, t, \Omega_0), \\
p_{\text{ref},12}^+(\mathbf{x}, t, \Omega_0) &= iK_0 \mathbf{F}_0^+ \\
&\cdot \mathbf{A}_{\text{ref},12}^+(x + x_{10} - v_0 t, y + \xi_0, z + z_0) \\
&\times P_{\text{ref},12}^+(\mathbf{x}, t, \Omega_0), \\
p_{\text{rad},12}^-(\mathbf{x}, t, \Omega_0) &= iK_0 \mathbf{F}_0^- \\
&\cdot \mathbf{A}_{\text{rad},12}^-(x - x_{20} + v_0 t, y - \xi_0, z - z_0) \\
&\times P_{\text{rad},12}^-(\mathbf{x}, t, \Omega_0), \\
p_{\text{ref},12}^-(\mathbf{x}, t, \Omega_0) &= iK_0 \mathbf{F}_0^- \\
&\cdot \mathbf{A}_{\text{ref},12}^-(x - x_{20} + v_0 t, y - \xi_0, z + z_0) \\
&\times P_{\text{ref},12}^-(\mathbf{x}, t, \Omega_0), \\
p_{\text{rad},I}^+(\mathbf{x}, t, \Omega_0) &= iK_0 \mathbf{F}_{0,I}^+ \\
&\cdot \mathbf{A}_{\text{rad},I}^+(x + x_0 - v_0 t, y + \xi_0, z - z_0) \\
&\times P_{\text{rad},I}^+(\mathbf{x}, t, \Omega_0), \\
p_{\text{ref},I}^+(\mathbf{x}, t, \Omega_0) &= iK_0 \mathbf{F}_{0,I}^+ \\
&\cdot \mathbf{A}_{\text{ref},I}^+(x + x_0 - v_0 t, y + \xi_0, z + z_0) \\
&\times P_{\text{ref},I}^+(\mathbf{x}, t, \Omega_0), \\
p_{\text{rad},II}^+(\mathbf{x}, t, \Omega_0) &= iK_0 \mathbf{F}_{0,II}^+ \\
&\cdot \mathbf{A}_{\text{rad},II}^+(x - \xi_0, y + s^+ - v_0 t, z - z_0) \\
&\times P_{\text{rad},II}^+(\mathbf{x}, t, \Omega_0), \\
p_{\text{ref},II}^+(\mathbf{x}, t, \Omega_0) &= iK_0 \mathbf{F}_{0,II}^+ \\
&\cdot \mathbf{A}_{\text{ref},II}^+(x - \xi_0, y + s^+ - v_0 t, z + z_0) \\
&\times P_{\text{ref},II}^+(\mathbf{x}, t, \Omega_0), \\
p_{\text{rad},II}^-(\mathbf{x}, t, \Omega_0) &= iK_0 \mathbf{F}_{0,II}^- \\
&\cdot \mathbf{A}_{\text{rad},II}^-(x - \xi_0, y - y_0 + v_0 t, z - z_0) \\
&\times P_{\text{rad},II}^-(\mathbf{x}, t, \Omega_0),
\end{aligned} \tag{33}$$

$$\begin{aligned}
p_{\text{ref},II}^-(\mathbf{x}, t, \Omega_0) &= iK_0 \mathbf{F}_{0,II}^- \\
&\cdot \mathbf{A}_{\text{ref},II}^-(x - \xi_0, y - y_0 + v_0 t, z + z_0) \\
&\times P_{\text{ref},II}^-(\mathbf{x}, t, \Omega_0), \\
p_{\text{rad},I}^-(\mathbf{x}, t, \Omega_0) &= iK_0 \mathbf{F}_{0,I}^- \\
&\cdot \mathbf{A}_{\text{rad},I}^-(x - s^- + v_0 t, y + \xi_0, z - z_0) \\
&\times P_{\text{rad},I}^-(\mathbf{x}, t, \Omega_0), \\
p_{\text{ref},I}^-(\mathbf{x}, t, \Omega_0) &= iK_0 \mathbf{F}_{0,I}^- \\
&\cdot \mathbf{A}_{\text{ref},I}^-(x - s^- + v_0 t, y + \xi_0, z + z_0) \\
&\times P_{\text{ref},I}^-(\mathbf{x}, t, \Omega_0), \\
p_{\text{rad},III}^\pm(\mathbf{x}, t, \Omega_0) &= iK_0 \mathbf{F}_{0,III}^\pm \\
&\cdot \mathbf{A}_{\text{rad},III}^\pm(\boldsymbol{\xi}, z - z_0, t) \\
&\times P_{\text{rad},III}^\pm(\mathbf{x}, t, \Omega_0), \\
p_{\text{ref},III}^\pm(\mathbf{x}, t, \Omega_0) &= iK_0 \mathbf{F}_{0,III}^\pm \\
&\cdot \mathbf{A}_{\text{ref},III}^\pm(\boldsymbol{\xi}, z + z_0, t) \\
&\times P_{\text{ref},III}^\pm(\mathbf{x}, t, \Omega_0),
\end{aligned} \tag{33} \text{Cont.}$$

and

$$\begin{aligned}
\mathbf{F}_0^\pm(\mathbf{x}, t) &= (\pm F_{0x}, \pm F_{0y}, F_{0z}), \\
\mathbf{F}_{0,I}^\pm(\mathbf{x}, t) &= (\pm F_{0x}, \pm F_{0y}, F_{0z}), \\
\mathbf{F}_{0,II}^\pm(\mathbf{x}, t) &= (\mp F_{0x}, \pm F_{0y}, F_{0z}), \\
\mathbf{F}_{0,III}^\pm(\mathbf{x}, t) &= (\mp F_{0\xi}, \pm F_{0\theta}, F_{0z}), \\
\mathbf{A}_{\text{rad},12}^\pm(\mathbf{x}, t) &= \{A_x^\pm(\mathbf{x}), A_y^\pm(\mathbf{x}), A_z^\pm(\mathbf{x}, t)\}, \\
\mathbf{A}_{\text{ref},12}^\pm(\mathbf{x}, t) &= \{A_x^\pm(\mathbf{x}), A_y^\pm(\mathbf{x}), -A_z^\pm(\mathbf{x}, t)\}, \\
\mathbf{A}_{\text{rad},S}^\pm(\mathbf{x}, t) &= \{A_{x,S}^\pm(\mathbf{x}), A_{y,S}^\pm(\mathbf{x}), A_{z,S}^\pm(\mathbf{x}, t)\}, \\
\mathbf{A}_{\text{ref},S}^\pm(\mathbf{x}, t) &= \{A_{x,S}^\pm(\mathbf{x}), A_{y,S}^\pm(\mathbf{x}), -A_{z,S}^\pm(\mathbf{x}, t)\} \\
&\quad (S = I, II, III)
\end{aligned} \tag{34}$$

with

$$\begin{aligned}
A_\alpha^\pm(\mathbf{x}, t) &= -\frac{1}{\alpha_{xy}^\pm} \left\{ M_{w\alpha}^\pm - \frac{r_\alpha^\pm(\boldsymbol{\xi})}{R_w^\pm(\mathbf{x})} \left[ 1 - \frac{1}{iK^\pm R_w^\pm(\mathbf{x})} \right] \right\}, \\
A_z^\pm(\mathbf{x}, t) &= \frac{z}{R_w^\pm(\mathbf{x})} \left[ 1 - \frac{1}{iK^\pm R_w^\pm(\mathbf{x})} \right], \\
A_{\alpha,\beta}^\pm(\mathbf{x}) &= -\frac{1}{\alpha_{xy,\beta}^\pm} \left\{ M_{w\alpha,\beta}^\pm - \frac{r_{\alpha,\beta}^\pm(\boldsymbol{\xi})}{R_{w\alpha,\beta}^\pm(\mathbf{x})} \right. \\
&\quad \left. \times \left[ 1 - \frac{1}{iK_{0,\beta}^\pm R_{w\alpha,\beta}^\pm(\mathbf{x})} \right] \right\}, \\
A_{z,\beta}^\pm(\mathbf{x}) &= \frac{z}{R_{w\alpha,\beta}^\pm(\mathbf{x})} \left[ 1 - \frac{1}{iK_{0,\beta}^\pm R_{w\alpha,\beta}^\pm(\mathbf{x})} \right],
\end{aligned} \tag{35}$$

$$A_{\alpha,III}^{\pm}(\mathbf{x}, t) = -\frac{1}{\alpha_{xy}} \left\langle M_{wx} - \left\{ \frac{r_{\alpha}^{\pm}(\boldsymbol{\xi}, t)}{R_{w,III}^{\pm}(\mathbf{x}, t)} \right. \right. \\ \left. \left. - \{1 \mp M_w \varepsilon \sin[\theta_0^{\pm}(t) - \theta_w]\} \right. \right. \\ \left. \left. \pm \varepsilon r_{\alpha} [\sin \theta_0^{\pm}(t), \cos \theta_0^{\pm}] \right. \right. \\ \left. \left. \times \left[ 1 - \frac{1}{iK_{0,III}^{\pm} R_{w,III}^{\pm}(\mathbf{x}, t)} \right] \right\} \right\rangle,$$

$$A_{z,III}^{\pm}(\mathbf{x}, t) = \frac{z}{R_{w,III}^{\pm}(\mathbf{x}, t)} \{1 \mp M_w \varepsilon \sin[\theta_0^{\pm}(t) - \theta_w]\} \\ \times \left[ 1 - \frac{1}{iK_{0,III}^{\pm} R_{w,III}^{\pm}(\mathbf{x}, t)} \right],$$

$$r_x^{\pm}(\boldsymbol{\xi}) = \alpha_y x + \beta_{xy}^{\pm} y,$$

$$r_y^{\pm}(\boldsymbol{\xi}) = \beta_{xy}^{\pm} x + \alpha_x^{\pm} y,$$

$$r_{x,I}^{+}(\boldsymbol{\xi}) = \alpha_y x + \beta_{xy,I}^{+} y,$$

$$r_{y,I}^{+}(\boldsymbol{\xi}) = \beta_{xy,I}^{+} x + \alpha_x^{+} y,$$

$$r_{x,II}^{+}(\boldsymbol{\xi}) = \alpha_y^{+} x + \beta_{xy,II}^{+} y,$$

$$r_{y,II}^{+}(\boldsymbol{\xi}) = \beta_{xy,II}^{+} x + \alpha_x^{+} y,$$

$$r_{x,I}^{-}(\boldsymbol{\xi}) = \alpha_y x + \beta_{xy,I}^{-} y,$$

$$r_{y,I}^{-}(\boldsymbol{\xi}) = \beta_{xy,I}^{-} x + \alpha_x^{-} y,$$

$$r_{x,II}^{-}(\boldsymbol{\xi}) = \alpha_y^{-} x + \beta_{xy,II}^{-} y,$$

$$r_{y,II}^{-}(\boldsymbol{\xi}) = \beta_{xy,II}^{-} x + \alpha_x^{-} y,$$

$$r_{\alpha}^{\pm}(\boldsymbol{\xi}, t) = r_{\alpha}(\boldsymbol{\xi} - \boldsymbol{\xi}') \Big|_{\xi'=\xi_0, \theta'=\theta_0^{\pm}(t)} \\ (\alpha = x, y; \quad \beta = I, II),$$

$$M_{wy}^{\pm} = M_{wy}. \quad (35)_{\text{Cont.}}$$

## References

1. ACHENBACH J.D. (1973), *Wave propagation in elastic solids*, North-Holland Publ. Co., Amsterdam, London; Amer. Elsevier Publ. Co., Inc., New York.
2. CHEVALLIER E., CAN A., NADJI M., LECLERCQ L. (2009a), *Improving noise assessment at intersections by modeling traffic dynamics*, Transportation Research. Part D: Transport and Environment, **14**, 2, 100–110.
3. CHEVALLIER E., LECLERCQ L., LELONG J., CHATAGNON R. (2009b), *Dynamic noise modeling at roundabouts*, Applied Acoustics, **70**, 5, 761–770.
4. CHODUR J. (2007), *Functioning of road intersections in the conditions of traffic variability* [in Polish], Tadeusz Kościuszko University of Technology Press, Cracow.
5. COVACIU D., TIMAR J., FLOREA D., COFARU C. (2013), *Considerations about the road traffic noise in a roundabout versus a signalized intersection*, Advances in Production, Automation and Transportation Systems: Proc. 6th Int. Conf. Manufacturing Eng., Quality and Production Systems (MEQAPS '13); Proc. 4th Int. Conf. on Automotive and Transportation Systems (ICAT '13), Brasov, Romania, June 1–3, 2013. Brasov, 349–354.
6. CYRIL A., KOSHY B.I. (2013), *Modelling of road traffic noise*, International Journal of Innovative Research in Sciences, Engineering and Technology, **2**, 1, 125–130.
7. ENGEL Z. (2001), *Protecting the environment from vibrations and noise* [in Polish], PWN, Warsaw.
8. FELSEN L., MARKUVITZ N. (1973), *Radiation and scattering of waves*, Prentice-Hall Inc., Englewood Cliffs, New Jersey.
9. FOTHERBY T. (2002), *Visual traffic simulation*, Individual Project; Final Report; MEng Computing Degree Rept.; Dept. Comp. Imperial College.
10. GUARNACCIA C. (2010), *Acoustical noise analysis in road intersections: a case study*, AMTA'10 Proc. 11th WSEAS Int. Conf. on Acoust. and Music: Theory and Appl., Iasi, June 13–15, 2010, Stevens Point, Wisconsin, 208–215.
11. HALLIWELL R.E. (1980), *Effect of stoplights on traffic noise*, Canadian Acoustics, **8**, 2, 22–31.
12. JAHANDAR N., HOSSEINPOUR A., SAHRAEI M.A. (2012), *Traffic noise under stop and go conditions in intersections – a case study*, World Academy of Science, Engineering and Technology, **62**, 465–468.
13. JOHNSON M.T. (2014), *Synthesis of roundabout design and operations with flared entries*, TRB 4th Annu. Meeting Compendium of Papers/Transportation Res. Board. Washington, 18 p.
14. KECS W., TEODORESCU P.P. (1978), *Introduction in theory of distributions with applications in technique* [in Russian], Mir, Moscow.
15. KETTEL P., ENGSTRÖM G., WIBERG N.-E. (2005), *Coupled hydro-mechanical wave propagation in road structures*, Computer and Structures, **83**, 21–22, 1719–1729.
16. MAKAREWICZ R., GOLEBIEWSKI R. (2007), *Modeling of the roundabout noise impact*, Journal of the Acoustical Society of America, **122**, 2, 860–868.
17. MAKAREWICZ R., KOKOWSKI P. (2007), *Prediction of noise changes due to traffic speed control*, Journal of the Acoustical Society of America, **122**, 4, 2074–2081.
18. MOHYLA I.A., DYAK M.A., SHVARYK I.YE. (2013), *The adaptive algorithm for traffic control at signalized T-intersection and its effectivity* [in Ukrainian], Visnyk of Donetsk Academy of Motor Transport, 1, 61–68.
19. MORSE P.M., INGART K.U. (1968), *Theoretical acoustics*, McGraw-Hill Book Co., New York.
20. MÜLLER G., MÖSER M. [Eds.] (2013), *Handbook of engineering acoustics*, Springer, Heidelberg; New York; Dordrecht; London.
21. NAMIKAWA Y., YOSHINAGA H., TAJIKA T., OSHINO Y., YOSHIHISA K., YAMAMOTO K. (2010), *Methods for predicting noise in the vicinity of signalized intersections*, Acoustical Science and Technology, **31**, 1, 87–97.

22. PIDDUBNIAK O., PIDDUBNIAK N. (2010), *Sound radiation from a roundabout*, Archives of Acoustics, **35**, 3, 437–456.
23. PIDDUBNIAK O., PIDDUBNIAK N., KRASNYK O. (2013), *Sound radiation from T junction of city roads*, Direct and Inverse Problems of Electromagnetic and Acoustic Wave Theory: Proc. 18th Int. Seminar/Workshop, Lviv, Sept. 23–26, 2013. Lviv, 226–232.
24. PIDDUBNIAK O., PIDDUBNIAK N., KUREK Ł., DUJKA M. (2009a), *Sound car radiation from crossroad*, Direct and Inverse Problems of Electromagnetic and Acoustic Wave Theory: Proc. 14th Int. Seminar/Workshop, Lviv, Sept. 21–24, 2009. Lviv, 261–266.
25. PIDDUBNIAK O., PIDDUBNIAK N., KUSIAK K. (2014), *Mathematical modeling of sound generation from Y junction of city roads*, Direct and Inverse Problems of Electromagnetic and Acoustic Wave Theory: Proc. 19th Int. Seminar/Workshop, Tbilisi, Sept. 22–25. Tbilisi, 168–173.
26. PIDDUBNIAK O., PIDDUBNIAK N., MAĐRA M. (2012a), *Sound radiation from roadway with a right-angle winding*, Direct and Inverse Problems of Electromagnetic and Acoustic Wave Theory: Proc. 17th Int. Seminar/Workshop, Tbilisi, Sept. 24–27, 2012. Tbilisi, 188–194.
27. PIDDUBNIAK O., PIDDUBNIAK N., TEODORCZYK T., ABRAMCZYK J. (2009b), *Radiation of roadway noise in windy conditions*, Direct and Inverse Problems of Electromagnetic and Acoustic Wave Theory: Proc. 14th Int. Seminar/Workshop, Lviv, Sept. 21–24, 2009. Lviv, 253–260.
28. SYKES P., DREW H. (2011), *An integrated assessment approach for road traffic noise*, 16th JCT Traffic Signal Symp. and Exhibition, 21–22 Sept. 2011, Univ. Warwick, 1–13.
29. YOSHIHISA K., OSHINO Y., YAMAMOTO K., TACHIBANA H. (2004), *Road traffic noise prediction in the vicinity of signalized intersections in urban areas*, 18th Int. Congr. Acoust.: ICA 2004: “Acoust. Sci. and Technol. for Quality of Life”, 4–9 Apr. 2004, Kyoto, IV-3019-IV-3022.
30. ZHAO J., ZHANG X., CHEN Y. (2012), *A novel traffic-noise prediction method for non-straight roads*, Applied Acoustics, **73**, 3, 276–280.